4.1 Introduction

The present chapter emphasizes the synthesis methods and various characterization of the heterogeneous barium aluminum oxide ($BaAl_2O_4$) and potassium aluminum oxide ($K_2Al_2O_4$). The catalyst $BaAl_2O_4$ was synthesized by co-precipitation route while physicochemical route was adopted for the synthesis of $K_2Al_2O_4$. The physicochemical characteristics of synthesized catalysts were analyzed by various spectroscopic techniques such as Thermo-gravimetric (TG) - Differential thermal (DT) analysis, X-ray diffraction (XRD), attenuated total reflectance Fourier transform infrared spectroscopy (ATR-FTIR), high-resolution Scanning Electron Microscope (HRSEM), Energy Dispersive X-ray spectroscopy, Brunauer-Emmett-Teller (BET) surface area analyzer – Barrett-Joyner-Halenda (BJH) pore diameter analyzer and basicity of the catalysts were determined by Hammett indicator titration.

4.2 Synthesis of catalyst barium aluminum oxide ($BaAl_2O_4$)

The catalyst barium aluminum oxide ($BaAl_2O_4$) was prepared by aqueous co-precipitation method at constant pH and temperature using metal nitrate precursors as shown in Figure 4.1. Solution A was prepared by dissolving the specific amount of barium nitrate and aluminium nitrate nonahydrate in double distilled water (Ba: Al molar ratio equal to 1:2) and Solution B was ammonia solution (25%). During the synthesis process, solution B was slowly and drop-wise added into solution A at constant stirring of 700 rpm. The temperature was maintained at 40 ºC throughout the addition and the final pH was reached as 10-11. After complete addition of solution B, resultant suspension was aged for another 6 h under constant stirring to facilitate the selective growth of the precipitate phase. Subsequently, the above precipitate was filtered using Whatman filter paper (Grade 42).

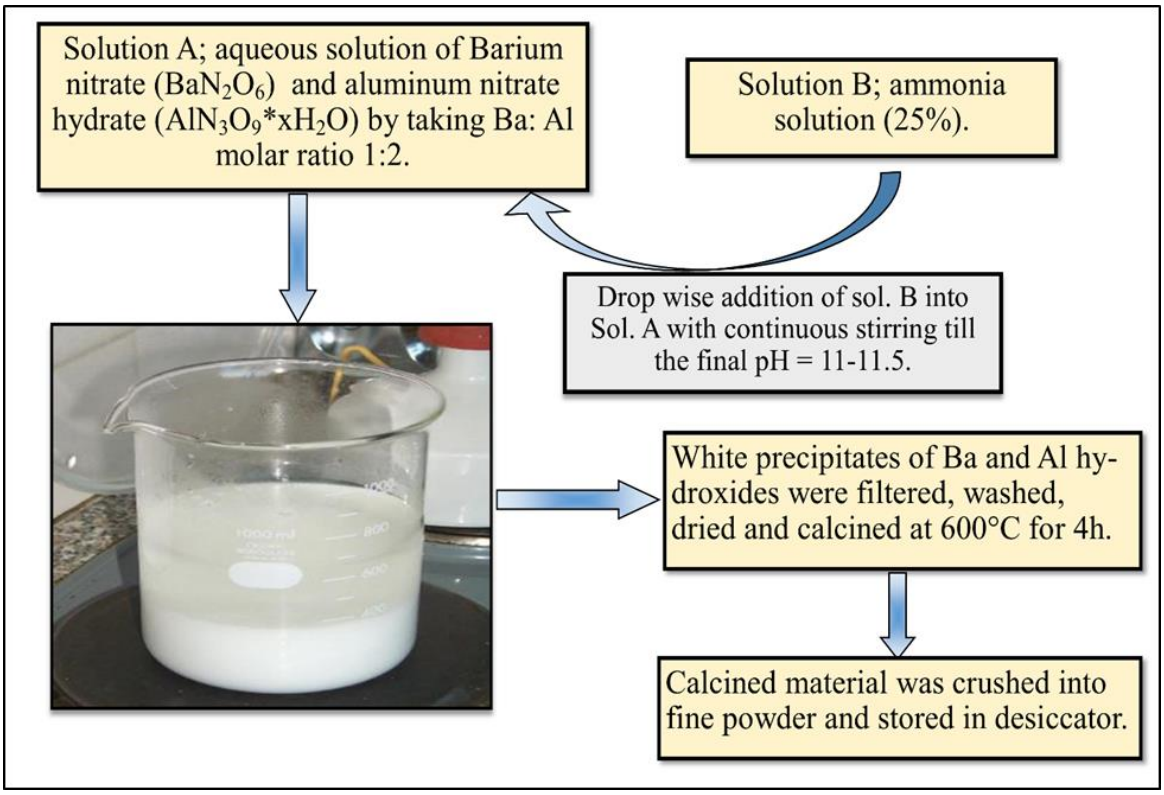

Figure 4.1 Schematic diagram of synthesis of $BaAl_2O_4$ by co-precipitation method

The complete precipitation of barium in form of barium hydroxide was ensured by silver nitrate test of filtrate. The obtained precipitate was washed with hot double distilled water and ethanol to remove any impurities. Afterwards, the solid sample was dried in a hot air oven at 100 °C for 12 h, and calcined in a muffle furnace in air flow at 600 °C for 4h. The resultant product was crushed in mortar-pestle and sieved to procure uniformly fine powder of catalyst. Finally, the catalyst was stored in a desiccator for further application.

4.3 Characterization of catalyst barium aluminum oxide ($BaAl_2O_4$)

4.3.1 Thermal characterization (TG-DTA)

The thermal characterization, including Thermo-gravimetric (TG) and Differential thermal (DT) analysis of synthesized uncalcined catalyst sample, were performed at a temperature range from room temperature to 900 °C and the results are shown in Figure 4.2. The TGA-DTA profile depicts four typical weight loss events in various temperature ranges in association with endothermic transformations. The first weight loss (5.94 wt%) of sample in the temperature range 50-130 °C could be attributed to the release of water and residual ammonia adsorbed on the surface of the material. The second weight loss step (15.08 wt%) corresponding to endothermic peak around 275 °C in DT curve is due to the pyrolysis of volatile organic matter such as nitrates from the precursors [Djoudi et al., 2012]. The final two successive, third and fourth endothermic transformations observed around 450 °C and 580 °C can be attributed to the decomposition of hydroxide phases formed during the precipitation into metal oxides and loss of 15.29 wt% and 13.01 wt% in TG curve, respectively. The TG results are in good agreement with the DT analysis as well as XRD. Above 600 °C, no change in weight observed in thermogram indicates the completion of calcination and crystallization reactions to form $BaAl_2O_4$ phase. Thus, 600 °C was chosen as calcination temperature [Fu et al., 2013].

4.3.2 XRD

X-ray powder diffraction is a reliable technique used to study the crystallographic characters such as structure, phase, preferred crystalline orientation and crystallite size. Figure 4.3 represents the typical diffractogram of as-prepared barium aluminum oxide ($BaAl_2O_4$).

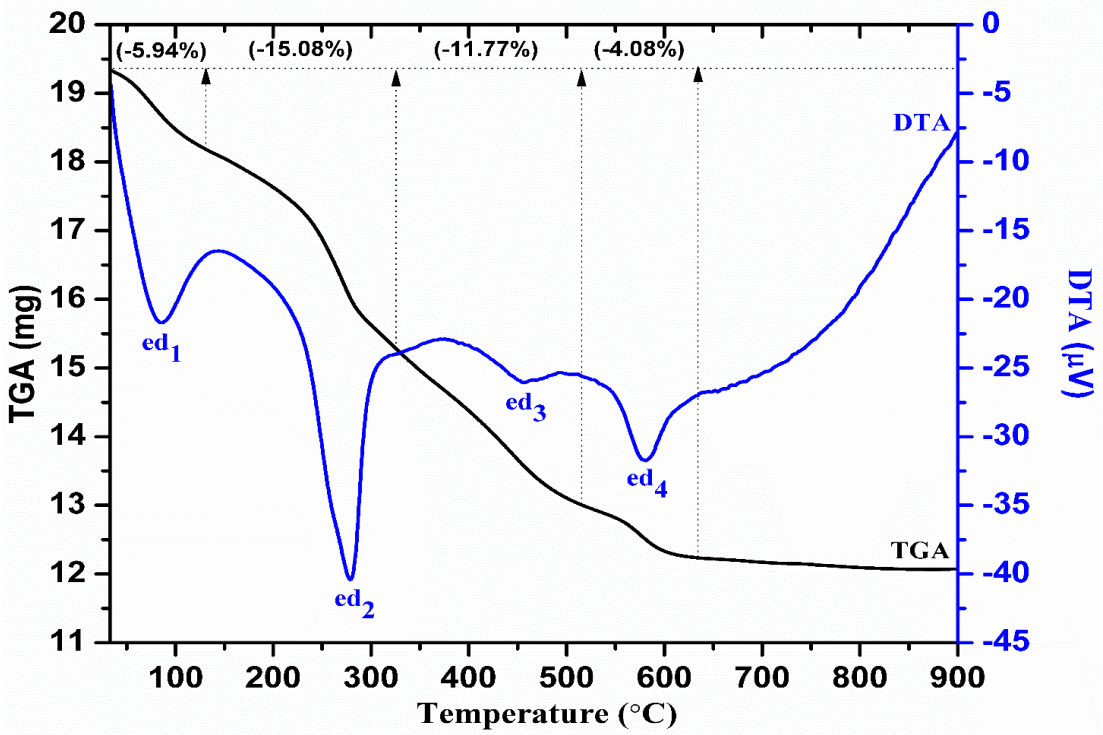

Figure 4.2 Thermal analysis (TGA-DTA) of uncalcined catalyst sample

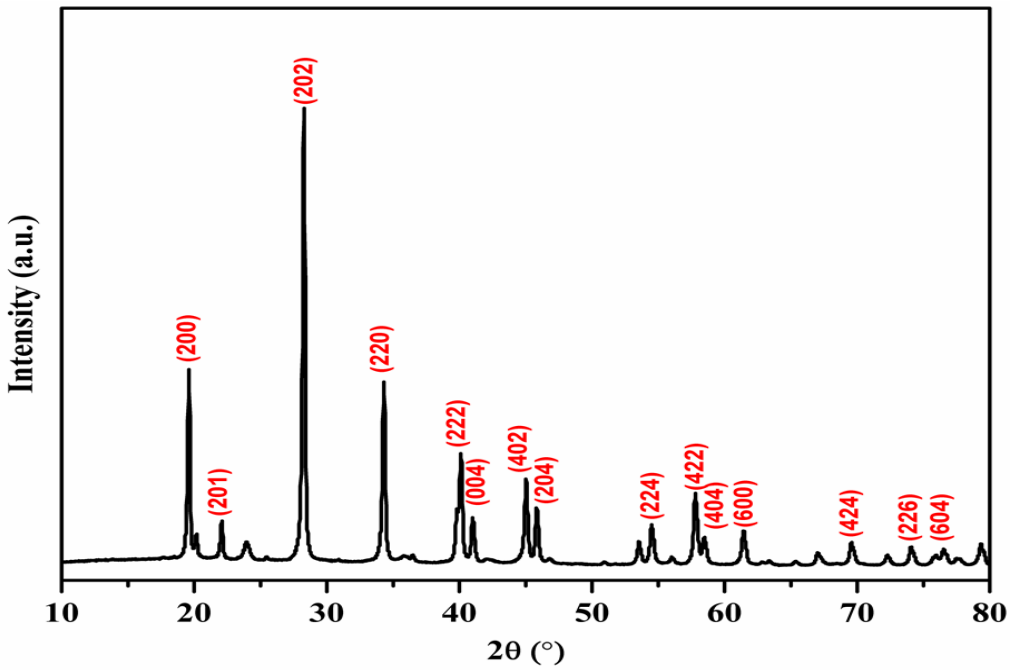

Figure 4.3 X-ray diffractogram (2θ = 10-80°) of the catalyst $BaAl_2O_4$ sample

The obtained diffractogram was matched with the Joint Committee on Powder Diffraction Standards (JCPDS) database. The apparent peaks at 2θ values (in degree) with crystal plane for 19.60° (2 0 0), 22.08° (2 0 1), 28.28° (2 0 2), 34.3° (2 2 0), 40.11° (2 2 2), 41.0° (0 0 4), 45.04° (4 0 2), 45.85° (2 0 4), 54.50° (2 2 4) and 57.81°(4 2 2) corresponding to the *d*-spacing 4.52, 4.0, 3.15, 2.60, 2.24, 2.19, 2.0, 1.97, 1.68, and 1.59 Å confirming the formation of barium aluminum oxide ($BaAl_2O_4$) JCPDS card no. 17-0306. The synthesized catalyst belongs to the hexagonal crystal system with P6322 space group [Mahmoudian et al., 2015]. The preferred orientation of $BaAl_2O4$ crystal was 28.28° (2 0 2) indicating crystal growth along the 2 0 2 direction. The apparent crystallite size of the catalyst was also calculated by using the Debye-Scherrer equation considering the intense diffraction peak and was found to be 75.02 nm [Battiston et al., 2014]

4.3.3 FT-IR

Fourier transform infrared spectroscopy (FTIR) is a distinctive technique employed to interpret the structural elucidations and surface functional species of the catalyst. In addition, it may also provide information about the quality and impurities present in the sample. The infrared spectrum of the barium aluminate $BaAl_2O_4$ hexagonal synthesized by co-precipitation route is illustrated in Figure 4.4. The prepared catalyst shows the two intense vibrational peaks in the range of 500-900 cm^{-1}, represents characteristics metal oxygen stretching frequencies associated with the vibration of diverse coordination states of Al metal [Torréns et al., 2013]. The vibrational peak at 677 cm^{-1} is attributed to the A1-O bond stretching in Al coordination states of AlO_4 tetrahedral group, whereas 503 cm^{-1} with very small shoulder peak at 561 cm^{-1}

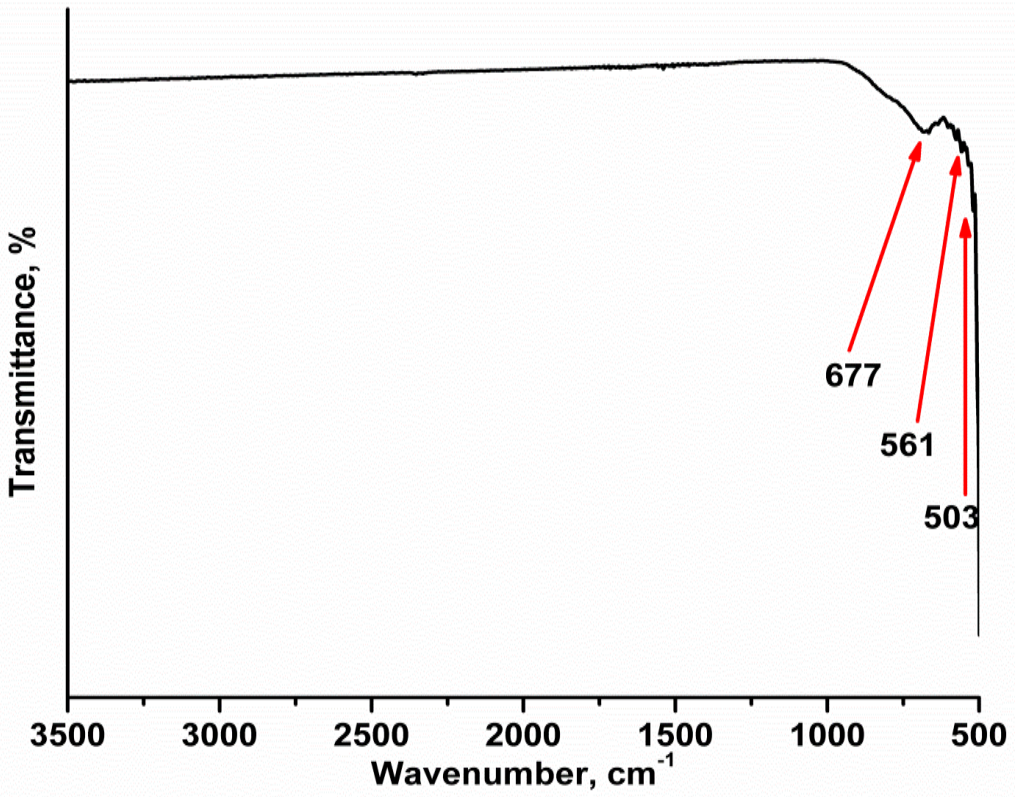

Figure 4.4 The FT-IR spectra of $BaAl_2O_4$ catalyst

could be due to $A1O_6$ octahedral group vibrations, respectively. No other peaks in spectra confirm the absence of any kind of impurities in $BaAl_2O_4$ [Tarte, 1967].

4.3.4 HR-SEM

The particle morphology and crystal structure of catalyst $BaAl_2O_4$ were recorded using High-Resolution Scanning Electron Microscopy (HRSEM) as shown in Figure 4.5. The magnified HRSEM micrograph of the catalyst sample shows that most of the particles exhibited flower-like shape with variable sizes. The diameter of the flower-like particles was estimated to be about 1-1.5 μm with well-defined petals. The petals of these structures are approx. 400-600 nm in length and 100-150 nm in the width at the middle [Kaur et al., 2018].

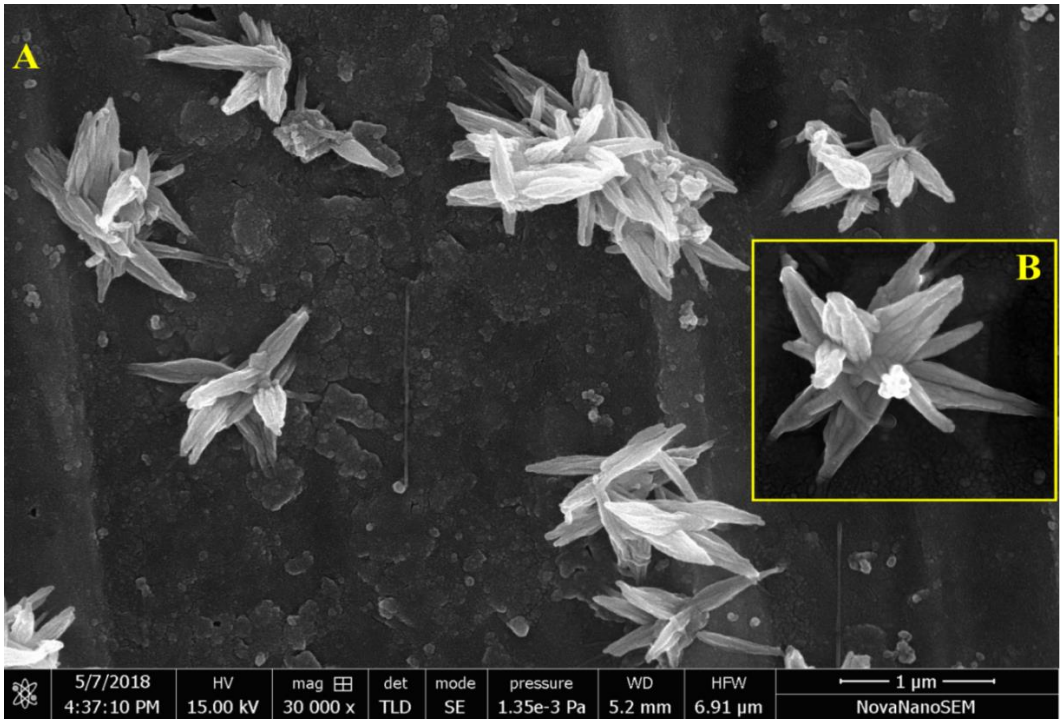

Figure 4.5 SEM micrographs of synthesized catalyst $BaAl_2O_4$ sample

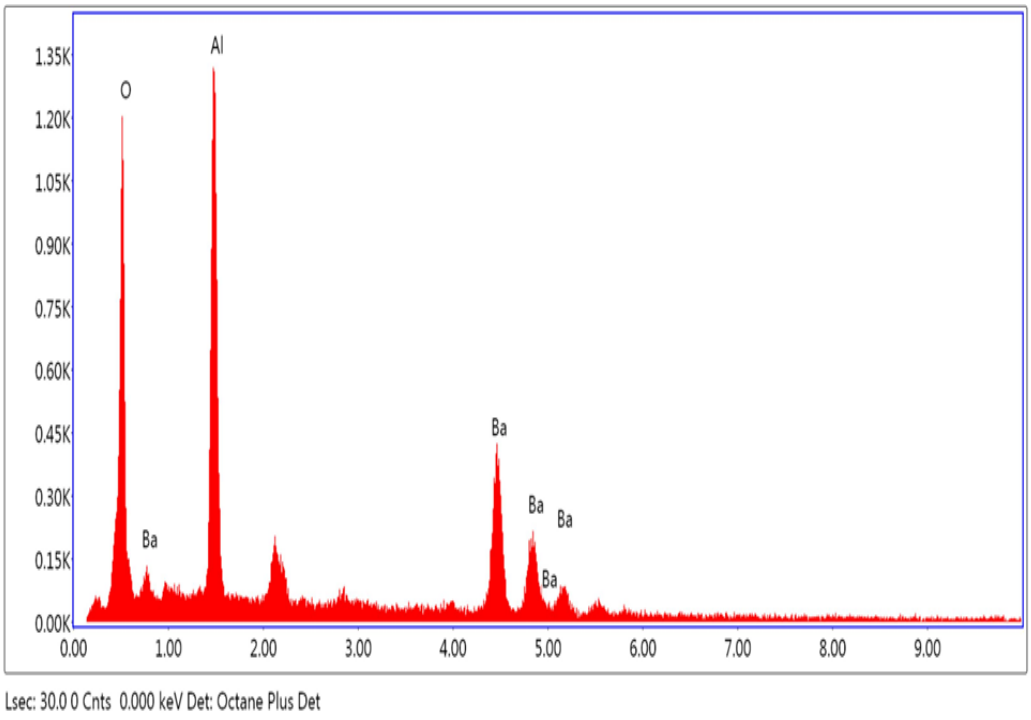

Figure 4.6 EDX spectrum of synthesized catalyst $BaAl_2O_4$ sample

4.3.5 EDX

The elemental composition of the catalyst $BaAl_2O_4$ sample was studied by Energy-dispersive X-ray spectroscopy (EDX) and obtained spectrum is shown in Figure 4.6. As shown in Figure 4.6, EDX spectrum validate the Ba, Al and O elements in catalyst sample in 13.94, 33.43, and 52.63 in atomic percent respectively. The obtained spectra also confirm the catalyst component $BaAl_2O_4$ with help of the atomic ratio which is nearly close to 1:2:4 [Vahid et al., 2018].

4.3.6 BET-BJH analysis

The textural characters surface area, pore size and pore volume of the catalyst $BaAl_2O_4$ play important roles in catalytic activity. The surface area of the catalyst sample was found to be 22.3 m^2/g, along with 0.01132 cm^3/g of total pore volume respectively. It was determined by N_2 physisorption plot between relative pressures (P/P_0) and quantity of adsorbed N_2. The adsorption and desorption curves were type IV with H1 isotherm hysteresis loops as classified by IUPAC, indicating the existence of mesoporous structure in the catalyst sample. On the basis of pore diameter, solids are classified as microporous when their diameter is up to 2 nm, mesoporous in the range of 2 to 50 nm and macroporous when the diameter is > 50 nm [Dehkordi and Ghasemi, 2012]. The pore diameter of catalyst was calculated from desorption isotherm branch by the BJH method and was found to be in a range of 1.22- 14.03 nm. The average pore size was 2.029 nm which implies the most of the pores present on catalyst surface were in mesoporous range. The mesoporous nature of the synthesized catalyst is an important aspect in reactions of large-sized molecule species (triglycerides) to diffusion on the catalyst surface [Salinas et al., 2018].

4.3.7 Basic strength and amount determination

To investigate the total basicity and basic strength distribution of the catalyst, the Hammett indicator test was carried out. The test results showed that catalyst changed the colour of bromothymol blue, phenolphthalein, 2, 4-dinitroaniline and 4-nitroaniline into their respective basic forms. This observation concluded that catalyst's basic strength lies in the range of 18.4 < H_ which is vital to catalyze transesterification reaction. As demonstrated in Table 4.1 catalyst can be considered as a strong base because it has mainly strong base sites {1.34 $mmolg^{-1}$(15< H_) and 2.18 $mmolg^{-1}$ (18.4< H_)} originated due to structural oxide (O^{2-}) component. Although, a very small medium base sites {.05 $mmolg^{-1}$ (7.2< H_) and 0.60 $mmolg^{-1}$ (9.3< H_)}were also presented on catalyst surface. It is important to note that difficulties related to diffusion of the indicator molecules into the pores of catalyst might occur in titration technique [Thitsartarn and Kawi, 2011].

Table 4.1 Basicity and base strength of synthesized catalyst $BaAl_2O_4$

Indicator	**Base strength**	**Observed colour (basic form)**	**Required amount of benzene carboxylic acid ($mmolg^{-1}$)**
Bromothymol blue	7.2	yellow to blue	0.03
Phenolphthalein	9.3	colourless to dark pink	0.57
2, 4-dinitroaniline	15	yellow to violet	1.34
4-nitroaniline	18.4	yellow to orange	2.18

4.4 Synthesis of catalyst potassium aluminum oxide ($K_2Al_2O_4$)

Physiochemical method was adopted for the synthesis of potassium aluminum oxide ($K_2Al_2O_4$). Briefly, calculated amount of alumina (Al_2O_3) and potassium carbonate (K_2CO_3) in 1:1 stoichiometric ratio was weighed and homogenized in a ball mill for 2 h using acetone. The resultant material was heat treated in presence of air at 950 ºC for 4 h in a muffle furnace and subsequently crushed and sieved to procure uniform powder form. The synthesized heterogeneous catalyst $K_2Al_2O_4$ was stored in desiccator for further application. Figure 4.7 depicts the schematic diagram of synthesis of $K_2Al_2O_4$ catalyst [Dai et al., 2015].

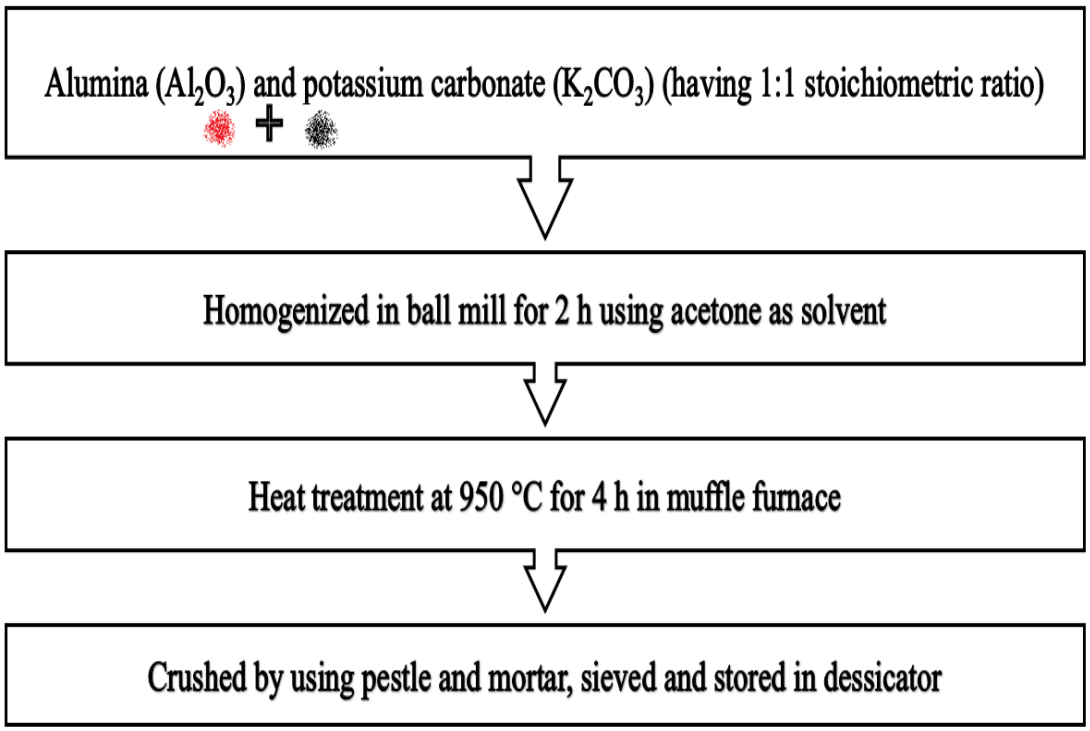

Figure 4.7 Schematic diagram of synthesis of $K_2Al_2O_4$ by physicochemical method

4.5 Characterization of the catalyst potassium aluminum oxide ($K_2Al_2O_4$)

4.5.1 Thermal characterization (TG-DTA)

Thermal characterization including thermo-gravimetric (TG)–Differential thermal (DT) analysis gives information about the thermal stability of the material at different temperatures. The experimental thermal decomposition curve in temperature range from room temperature to 1000 °C of the uncalcined sample is presented in Figure 4.8. From thermogram, it was observed that the total weight loss of 16.16% occurred in three weight loss events with endothermic transformations. First rapid weight loss of sample, about 5.22% in the temperature range 40-200 °C was due to evaporation of physically adsorbed water from the outer and internal surface of the sample. The second slow and third broad region weight losses of about 2.83 and 8.11%, respectively occurred in the range of 200 °C - 650 °C and 650 °C - 950 °C respectively with corresponding endothermic peaks in DT curve. This behaviour may be related to slow and fast release of carbon dioxide due to decomposition of starting material potassium carbonate. Thereafter, no further weight loss was in TG curve shows that 950 °C could be an appropriate temperature for calcination, where the stable phase, potassium aluminum oxide was obtained from the result of XRD pattern [Lukic et al., 2009; Wang et al., 2017; Rashtizadeh et al., 2014]. Here, to accomplish solid state reaction between reactant K_2CO_3 and Al_2O_3, diffusion or penetration within the phase along with chemical reaction is a desirable aspect. It is noteworthy that when calcination temperature reached to above near about 900 °C, K_2CO_3 exist as molten state. It may be assumed that molten K_2CO_3 is mobile species and it reacts with Al_2O_3 grain at the interface to give $K_2Al_2O_4$ as a product [Alonso et al., 2007; Lehman et al., 1998].

$$K_2CO_3 + Al_2O_3 \rightarrow K_2Al_2O_4 + CO_2\uparrow \quad (4.1)$$

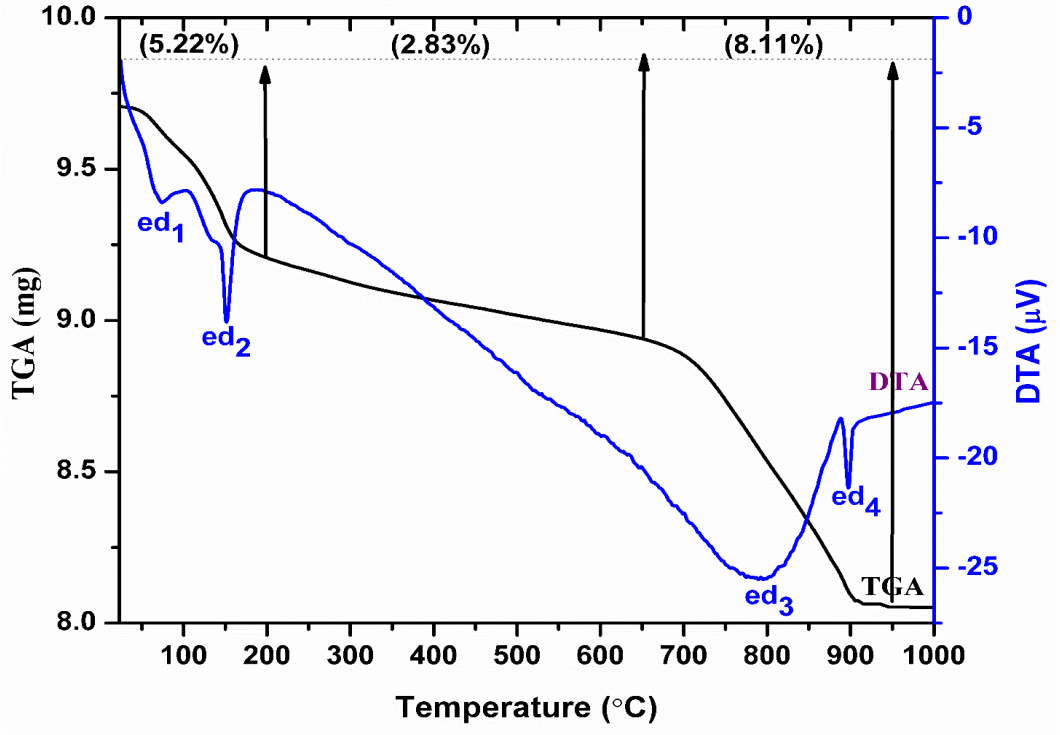

Figure 4.8 Thermal analysis (TGA-DTA) of uncalcined catalyst sample

4.5.2 XRD

Figure 4.9 presents the XRD pattern of as-synthesized potassium aluminum oxide, $K_2Al_2O_4$. The observed peaks in the diffractogram were compared with the Joint Committee on Powder Diffraction Standards (JCPDS) database and matched with the data reported in JCPDS file No. 0045-0849. The X-ray diffractogram of the sample shows the *d* values appearing at 3.09, 2.73, 2.61, 2.49, 2.41, 2.32, 2.22, 1.92, 1.57, 1.36 and 1.21 Å corresponding to the diffraction peaks at angular positions, 2θ (in degree) with crystal plane 28.87 (5 0 0), 32.72 (4 4 0), 34.31 (5 3 1), 35.99 (6 1 1), 37.28 (6 2 1), 38.64 (6 2 2), 40.47 (4 4 4), 47.09 (8 0 0), 58.60 (8 4 4), 68.88 (8 8 0) and 78.45 (12 4 0).

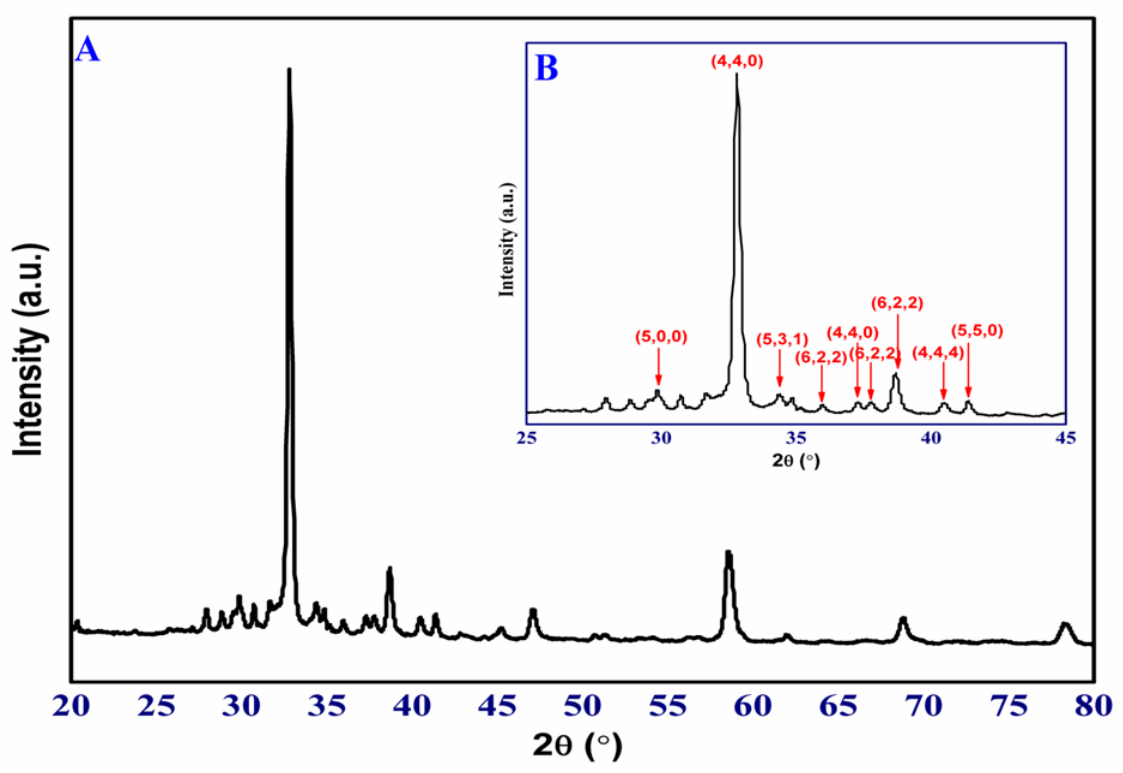

Figure 4.9 X-ray diffractogram (A) 2θ = 20-80° and (B) 2θ = 25-45° of potassium aluminum oxide synthesized by solid state method

These diffraction peaks were assigned to potassium aluminum oxide with cubic structure. In general, the diffraction peak 32.72° (4 4 0) is the preferred orientation for $K_2Al_2O_4$, indicating crystal growth along the (4 4 0) direction. No other minor phase diffraction peaks in diffractogram confirm the absence of impurities and high-level crystallinity of single phase $K_2Al_2O_4$. The apparent crystallite size of the as solid-state synthesized potassium aluminum oxide was also calculated by using the Debye-Scherrer equation by considering the intense diffraction peak (4 4 0). The crystallite size is found 34.19 nm [Vahid and Haghighi, 2017].

4.5.3 FT-IR

Attenuated total reflectance based Fourier transform infrared spectroscopy technique is a useful tool for the interpretation of surface functional groups. The infrared spectrum of synthesized catalyst potassium aluminum oxide is depicted in Figure 4.10. The catalyst sample exhibits low-intensity peaks in region 1300-1500 cm^{-1} which are attributed to stretching vibrations of -C-O bond due to adsorption of atmospheric CO_2 on a sample surface. Similarly, a weak out of plane and bending vibration was observed at 916 cm^{-1}. A broad and smooth adsorption band in region of 500-900 cm^{-1} reveals the presence of Al-O bond with diverse coordination of Al in the catalyst sample. The high vibration peak at 694 cm^{-1} is due to tetrahedral coordinated Al in Al-O bond and a low- intensity peak such as 536 $cm^{-1}$was due to octahedral coordination of Al [Torréns et al., 2013].

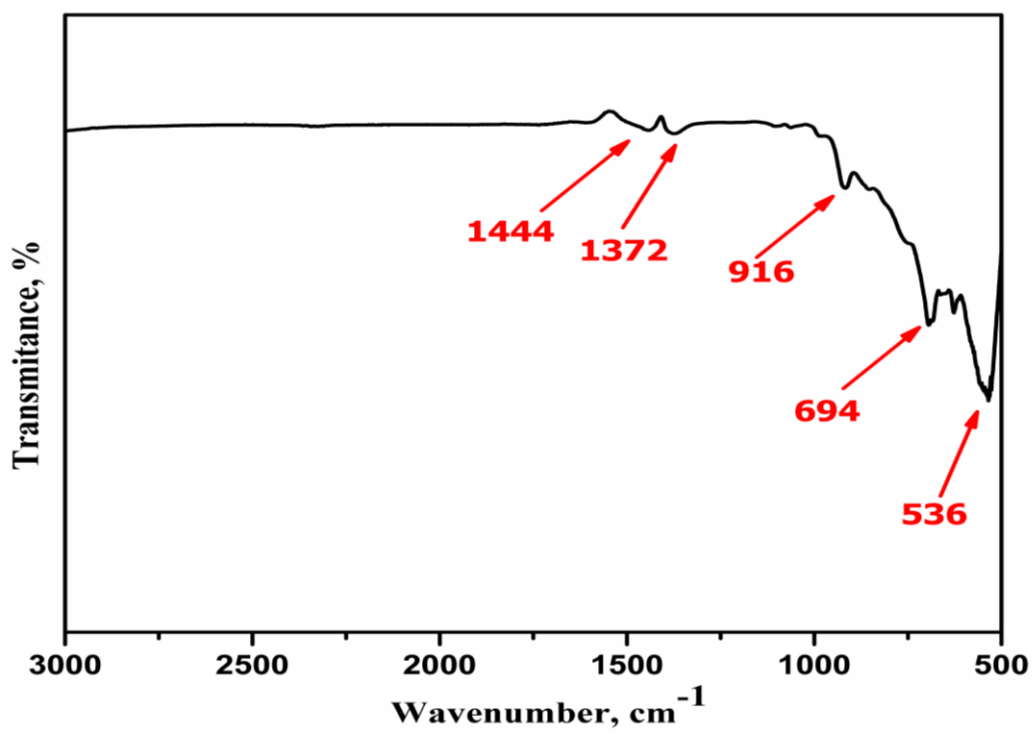

Figure 4.10 The FT-IR spectra of $K_2Al_2O_4$ catalyst

4.5.4 HR-SEM

The high-resolution Scanning Electron Microscopy (SEM) technique was used to study the crystal structure and morphology of particle of the synthesized catalyst. The SEM micrographs of the catalyst sample potassium aluminum oxide at low and high magnification are presented in Figure. 4.11(A) and (B) respectively. The magnified micrograph of the sample reveals that most of the catalyst particles were homogeneous and exhibited uniform spheroid morphology. The diameter of the catalyst particle is estimated to be approximately 2 μm as a result of solid state synthesis route in which interaction between guest and support molecules at high temperature is responsible for high activation of the catalyst. However, some agglomerations were also observed as a result of inter-particle interactions [Wan et al., 2014; Dang et al., 2013].

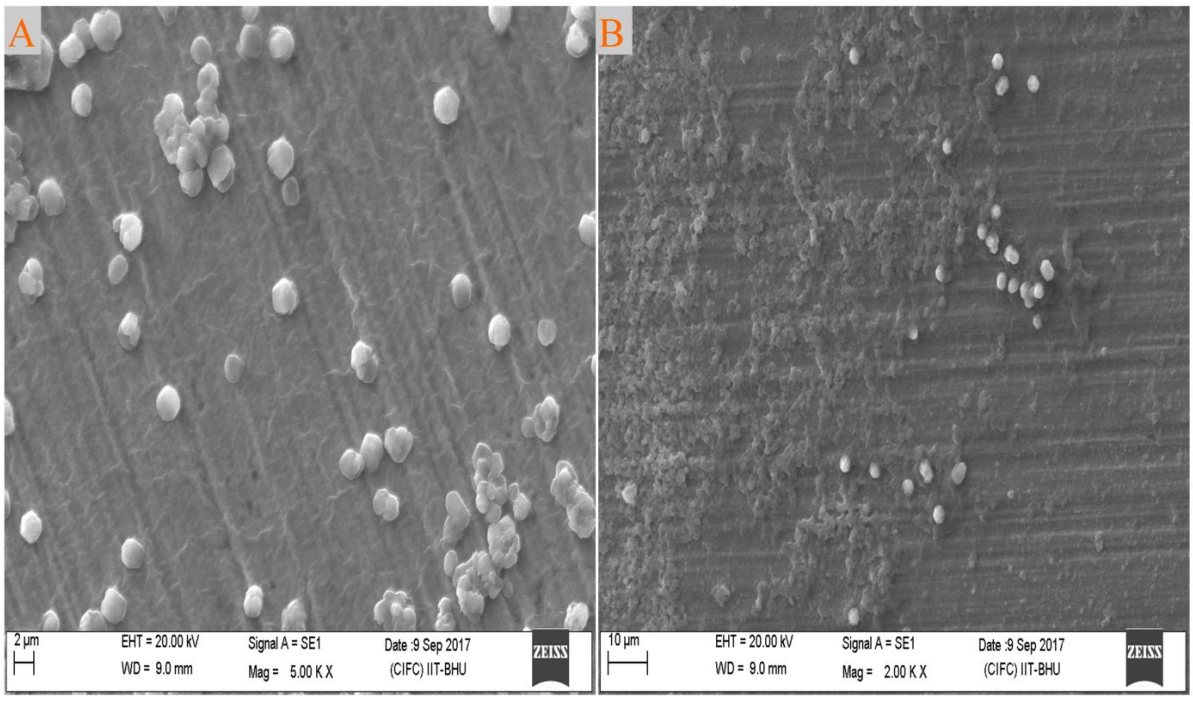

Figure 4.11 (A) Lower and (B) higher magnification SEM micrographs of the synthesized catalyst $K_2Al_2O_4$

4.5.5 EDX

Elemental analysis of as-synthesized catalyst $K_2Al_2O_4$ was verified by Energy-dispersive X-ray spectroscopy (EDX) and the obtained data validated the composition of the sample as shown in Figure 4.12. The EDS pattern shows that the average atomic percentage of K, Al and O is found 12.95, 13.96 and 29.29%, respectively. It also reveals that the catalyst is composed of K, Al and O with an atomic ratio close to 1:1:2, confirming that the catalyst component is $K_2Al_2O_4$. The Cu peak in EDX pattern is due to the copper substrate itself [Feyzi and Shahbazi, 2017].

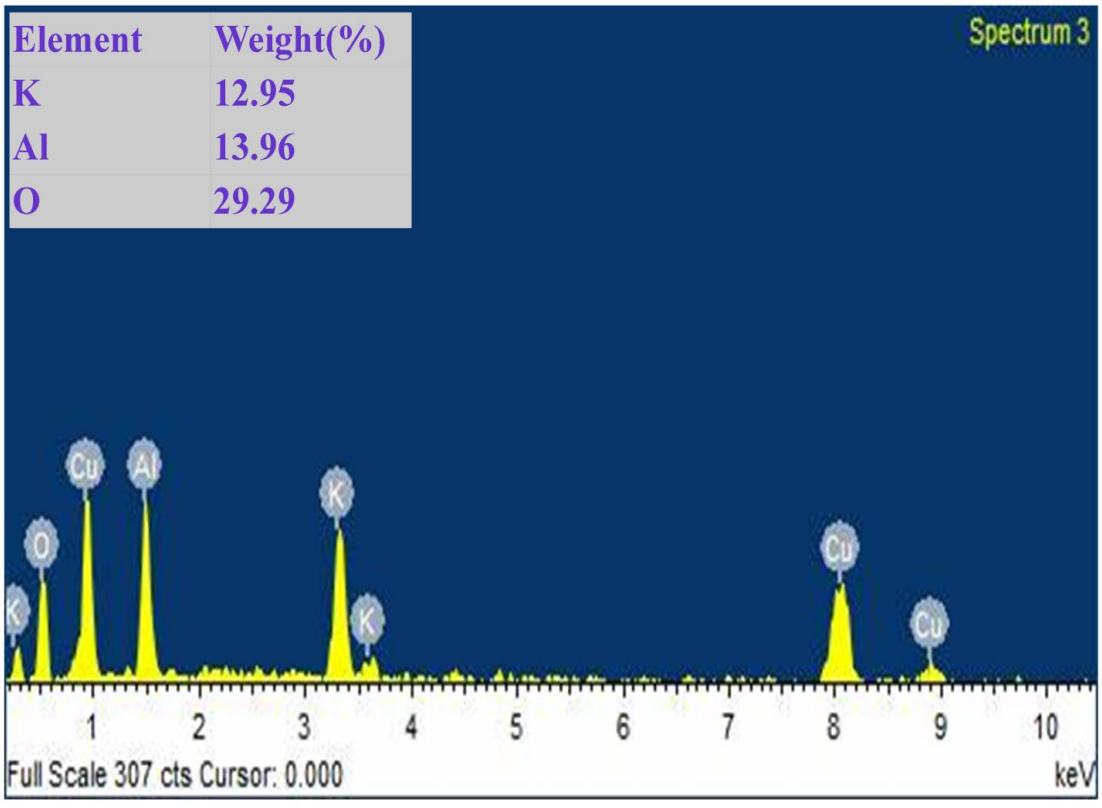

Figure 4.12 EDX spectrum of the catalyst $K_2Al_2O_4$

4.5.6 BET-BJH analysis

The information regarding textural characteristics such as surface area, pore size and pore volume of the synthesized catalyst via solid-state method was evaluated by means of BET-BJH method. The surface area of the catalyst was determined from the N_2 adsorption-desorption profile, plotted between relative pressure (P/P_0) versus quantity of adsorbed N_2 and was found to be a characteristics type IV curve with H1 loop that represents the mesoporous nature of materials. The single point surface area and total pore volume of synthesized catalyst were found to be 5.86 m^2/g and 0.1635cm^3/g, respectively. The pore diameter of the sample was determined from the desorption isotherm branch by the BJH model, which reveals a broad pore size distribution having pore diameter ranges from 3–100 nm indicating mesoporous (2-50 nm) and macroporous (>50 nm) nature of the catalyst [Veiga et al., 2016]. The small mesopores on the surface of catalyst are similar in size to the molecular dimensions of a typical triglyceride (5 nm) which is responsible for the high catalytic activity in the transesterification reaction. This may be due to the superior mass-transport of the bulky triglycerides and the greater accessibility of catalyst active site [Tantirungrotechai et al., 2011].

4.5.7 Basic strength and amount determination

The basic strength of the catalyst $K_2Al_2O_4$, was determined by Hammett titration method. The activity of a catalyst for the catalysis in transesterification reaction is related to its basic strengths. The higher base strengths of the catalyst could be responsible for the higher biodiesel conversion. Bromothymol blue, phenolphthalein, 2, 4-dinitroaniline and 4-nitroaniline were used to measure basic site strength and catalyst could change the respective colours of all these indicators into their basic form. This observation suggested that the catalyst has strong basic

Table 4.2. Basicity and base strength of catalyst $K_2Al_2O_4$

Indicator	**H_**	**Observed colour**	**Required amount of benzene carboxylic acid (mmolg^{-1})**
bromothymol blue	7.2	yellow to blue	0.05
Phenolphthalein	9.3	colourless to dark pink	0.60
2, 4-dinitroaniline	15	yellow to violet	1.49
4-nitroaniline	18.4	yellow to orange	2.23

sites with the basic strength of 18.4 < H_. Results of basic strength (H_) and amount determination tests are tabulated in Table 4.2. According to the results, 4.37 mmol amount of total basic sites with the basic strength of 18.4 < (H_) are present on the catalytic surface (per 1 g). These sites may be Lewis base in form of oxide ions which are attached on the surface of catalyst [Gao et al., 2015]. Therefore, all these results imply that the catalyst $K_2Al_2O_4$ would have enough Lewis basic strength to catalyze the transesterification reaction. However, it is important to note that this titration technique remains controversial due to solvent-support interactions and accessibility of probe molecule into pores [Thitsartarn and Kawi, 2011]

4.6. Conclusion

Heterogeneous base catalysts $BaAl_2O_4$ and $K_2Al_2O_4$ were synthesized by co-precipitation and physicochemical route and characterized by various spectroscopic techniques. The thermal characterization TGA-DTA reveal the thermal stability of synthesized catalyst samples, $BaAl_2O_4$ and $K_2Al_2O_4$ at 600 °C and 950 °C as calcination temperatures and XRD data well supported the formation of single crystalline phases of catalyst samples. The crystallite size of

synthesized catalysts $BaAl_2O_4$ and $K_2Al_2O_4$ were found to be 75.02 nm and 34.19 nm respectively. The particle morphology was confirmed by HRSEM analysis and $BaAl_2O_4$ catalyst had flower shape morphology whereas $K_2Al_2O_4$ has spherical morphology. The EDX spectra of catalysts confirm the respective composition of synthesized catalyst samples. The surface area and pore diameter were determined by BET-BJH analysis and were found to be 22.3 m^2/g and 2.029 nm for $BaAl_2O_4$ and 5.86 m^2/g and 5.0 nm for $K_2Al_2O_4$ catalyst respectively. Both the catalyst samples were mesoporous in nature. The catalysts $BaAl_2O_4$ and $K_2Al_2O_4$ have high basicity i.e. 4.12 $mmolg^{-1}$ and 4.37 $mmolg^{-1}$ and can be applied as heterogeneous base catalyst in transesterification reaction,